Original papers
Advanced structural materials, materials for extreme conditions

УДК 620.3 DOI: 10.17277/jamt-2026-11-02-118-128

The influence of graphene oxide additives on the structure of graphite/boron nitride filler and tribological characteristics of anti-friction material

© Roman D. Balabanov[a]✉, Tatyana P. Dyachkova[a], Irina V. Gutnik[a], Nikolay A. Chapaksov[a], Elena A. Burakova[a]

[a] *Tambov State Technical University, Bld. 2, 106/5, Sovetskaya St., Tambov, 392000, Russian Federation*

✉ balabanoff98@gmail.com

Abstract. The influence of graphene oxide (GO) additives on the structure of the graphite/hexagonal boron nitride hybrid filler and the tribotechnical characteristics of anti-friction composites obtained on its basis was assessed. The nanocomposite preparation method included obtaining the filler (mixture) through mechanical activation of the components, hot mixing the mixture with high-temperature coal tar pitch, pressing, and high-temperature firing. To ensure hermetic sealing, the products were finally impregnated with a furfuryl alcohol solution, followed by polymerization at 300°C. Mixture samples were analysed using thermogravimetry and X-ray diffraction analysis. It was found that with an increase in GO content to 2.80 wt.%, the thermal stability of the mixture increased, after which it began to decline. The dependence of the crystal structure parameters of the filler components (L_c and N) on the GO concentration also exhibited an extreme behaviour. A sample of the charge containing 1.64 wt. % graphene oxide is characterized by maximum L_c and N values for boron nitride and minimum values for the graphite component. Furthermore, the filler of this composition demonstrates maximum sorption capacity for pitch, which contributes to the formation of a high-density and durable material. The finished nanocomposite demonstrates gas permeability of less than 1×10^{-5} $cm^2 \cdot s^{-1}$ and compressive strength equal to 197.5 MPa, which is 1.5 times higher than that of an analogue (NIGRAN-V). Bench tests showed that due to the introduction of graphene oxide into the filler composition, wear intensity is reduced by 16 times compared to a sample based on an unmodified charge. The nanocomposite of the optimal composition remains hermetically sealed under extreme operating conditions and can serve as the basis for the creation of high-density and ultra-strong anti-friction materials suitable for use in sealed friction units of pump and compressor systems.

Keywords: graphene oxide; graphite; boron nitride; nanocomposite; sealed anti-friction material.

For citation: Balabanov RD, Dyachkova TP, Gutnik IV, Chapaksov NA, Burakova EA. The influence of graphene oxide additives on the structure of graphite/boron nitride filler and tribological characteristics of anti-friction material. *Journal of Advanced Materials and Technologies*. 2026;11(2):118-128. DOI: 10.17277/jamt-2026-11-02-118-128

Влияние добавок оксида графена на структуру наполнителя графит/нитрид бора и триботехнические характеристики антифрикционного материала

© Р. Д. Балабанов[a]✉, Т. П. Дьячкова[a], И. В. Гутник[a], Н. А. Чапаксов[a], Е. А. Буракова[a]

[a] *Тамбовский государственный технический университет, ул. Советская, 106/5, пом. 2, Тамбов, 392000, Российская Федерация*

✉ balabanoff98@gmail.com

Аннотация. Проведена оценка влияния добавок оксида графена (ОГ) на структуру гибридного наполнителя графит/гексагональный нитрид бора и триботехнические характеристики антифрикционных композитов, полученных на его основе. Методика приготовления нанокомпозитов включала получение наполнителя (шихты)

посредством механической активации компонентов, горячее смешивание шихты с высокотемпературным каменноугольным пеком, прессование и высокотемпературный обжиг. Для придания герметичности на финальной стадии изделия подвергались пропитке раствором фурфурилового спирта с последующей полимеризацией при 300 °C. Образцы шихты изучали методами термогравиметрии и рентгенофазового анализа. Установлено, что при увеличении содержания ОГ до 2,80 мас. % термическая стабильность шихты росла, а после снижалась. Зависимость параметров кристаллической структуры компонентов наполнителя (L_c и N) от концентрации ОГ также имела экстремальный характер. Образец шихты, содержащей 1,64 мас. % оксида графена, характеризовался максимальными значениями L_c и N для нитрида бора и минимальными – для графитового компонента. Кроме того, наполнитель данного состава демонстрировал максимальную сорбционную емкость по пеку, что способствует формированию высокоплотного и прочного материала. Готовый нанокомпозит демонстрировал газопроницаемость менее 1×10^{-5} см^2/с и прочность при сжатии, равную 197,5 МПа, что в 1,5 раза выше, чем у аналога (НИГРАН-В). В результате стендовых испытаний установлено, что за счет введения в состав наполнителя оксида графена интенсивность износа снижается в 16 раз по сравнению с образцом на основе немодифицированной шихты. Нанокомпозит оптимального состава остается герметичным в экстремальных условиях эксплуатации и может являться основой для создания высокоплотных и сверхпрочных антифрикционных материалов, пригодных для использования в герметичных узлах трения насосных и компрессорных систем.

Ключевые слова: оксид графена; графит; нитрид бора; нанокомпозит; герметичный антифрикционный материал.

Для цитирования: Balabanov RD, Dyachkova TP, Gutnik IV, Chapaksov NA, Burakova EA. The influence of graphene oxide additives on the structure of graphite/boron nitride filler and tribological characteristics of anti-friction material. *Journal of Advanced Materials and Technologies*. 2026;11(2):118-128. DOI: 10.17277/jamt-2026-11-02-118-128

1. Introduction

Ensuring high ductility of the anti-friction layer in dry friction units while simultaneously maintaining the material's structural density is an extremely difficult task [1, 2]. Typically, when producing self-lubricating composites, hermetic sealing is sacrificed for a low friction coefficient, making such materials unsuitable for use in modern high-pressure pump and compressor systems [3, 4]. Therefore, the development of composites with increased hermetic seal is critical for the reliable operation of sealing elements that prevent leaks in pumping units and compressors of modern technical devices.

The challenge of achieving high sealing performance combined with low friction remains unresolved, as traditional graphite materials often exhibit porosity that reduces their barrier properties [5], and the incorporation of conventional fillers does not always allow for the desired balance of mechanical and tribological characteristics to be achieved [6].

The advent of graphene and the subsequent development of methodologies for producing diverse nanostructures based on it have catalyzed research endeavors aimed at utilizing such materials in the field of tribology [7]. As demonstrated in studies [8, 9], there is considerable potential for the utilization of graphene oxide (GO) in anti-friction composites. The presence of oxygen-containing functional groups on GO facilitates chemical interaction with matrices and fillers, thereby ensuring uniform distribution of components throughout the composite volume and, consequently, enhancing the adhesive strength of the resultant material [10–12]. The utilization of GO additives in anti-friction materials has been demonstrated to reduce the coefficient of friction by forming a thin transfer film on the counterface, thereby significantly enhancing their sealing properties [13–14]. The low gas permeability of the resulting composites is ensured by the "labyrinth effect," which is effectively realized when the GO is uniformly distributed throughout the volume [15–17].

At the same time, according to [18], using graphene oxide alone as a filler generally fails to provide the required load-bearing capacity and thermal conductivity of the composite in the contact zone. To achieve a synergistic effect, combinations of GO with traditional solid lubricants – graphite [19] and hexagonal boron nitride (h-BN) [20–21] – can be used. Graphite provides high thermal conductivity and excellent lubricity in a wet environment, while boron nitride demonstrates high thermal stability and chemical inertness, performing well in conditions where graphite begins to oxidize [22–23]. The use of a mixture of fillers allows for the production of materials suitable for a wide range of operating conditions [24].

Most of the known studies concentrate on binary systems (graphene oxide–graphite or graphene oxide–boron nitride). However, combining graphite, boron nitride, and graphene oxide within a singular compositional system may help achieve maximum

effects [25]. The primary challenge in the formation of such materials stems from the agglomeration of dissimilar particles and the non-uniform distribution of nanoscale GO between graphite microparticles and h-BN [26–27]. The lack of fundamental knowledge regarding the mechanisms of interphase interaction in the "graphene oxide–boron nitride–graphite" ternary systems hinder the creation of materials with predictable tribotechnical properties [28–29]. Studies generally overlook the influence of filler morphology and orientation on the formation of tribolayers and structural integrity, despite the fact that these factors determine the sealing ability of the composite [30–33]. The objective of this research is to establish the patterns through which graphene additives influence the structure of "graphite–boron nitride" hybrid fillers and the tribological characteristics of the final composites.

2. Materials and Methods

2.1. Initial components

The starting components used to prepare the filler were MPG-7 synthetic graphite (apparent density 1.8 g·cm^{-3}) and hexagonal boron nitride (particle size less than 30 μm). A 1% aqueous suspension of graphene oxide (NanoTechCenter, Tambov) was used as a modifying additive. High-temperature coal tar pitch (softening point 148 °C) was used to form the composite matrix. The impregnating agent was a 95 % solution of furfuryl alcohol (Pallav Chemicals).

2.2. Sample preparation method

The sample preparation procedure included a mechanical activation step, carried out in a high-speed pulverizing machine (RT-N06SF, Rong Tsong Precision Technology, Taiwan), to ensure a homogeneous distribution of graphite throughout the charge. First, the graphite was ground into two fractions: one with particle sizes up to 30 μm and another ranging from 30 to 63 μm. Boron nitride and fine-fraction synthetic graphite (< 30 μm) were then loaded into the pulverizing machine at a mass ratio of 59:100. The nanomodifier content was varied between 0 and 3.66 wt. %. Mixing was performed at a blade rotation speed of 25,000 rpm for 30 s.

The resulting batch was subsequently combined with artificial graphite (particle size 30-63 μm) and pitch at a mass ratio of 1:2:2. This mixture was placed in a Z-blade mixer, heated to 230 °C, and processed for 30 min. After unloading and cooling, the mixture was ground in the pulverizing machine until a powder with particle sizes below 90 μm was obtained. The powder was then pressed in a 40-mm-diameter mold at 200 MPa using an AUTO M-PL 3890 (Carver, USA) press. The resulting cylindrical compacts (Fig. 1*a*) were finally fired at 900 °C.

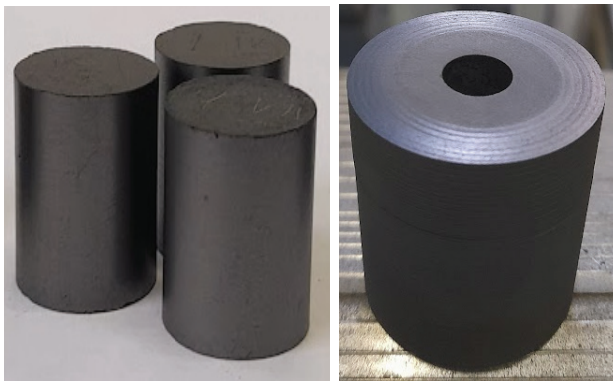

(a) *(b)*

Fig. 1. Photographs of cylindrical compacts (*a*) and a finished sample (*b*)

To ensure tight seal, the samples were additionally impregnated with a furfuryl alcohol solution, followed by polymerization at 300 °C. A photo of the finished sample is shown in Fig. 1*b*.

2.3 Evaluation of mixture adsorption capacity toward the binder and tribotechnical testing

The adsorption capacity of the mixture with respect to the pitch was determined by the difference in the optical density (OD) of the pitch solution in toluene before (D_0) and after (D_1) contact with the adsorbent, as measured on a UNICO 1201 (Unico, USA) photometric colorimeter using a 540 nm filter. Using a calibration curve, the concentrations (mg·mL^{-1}) of pitch C_0 and C_1 corresponding to the optical densities D_0 and D_1 were determined. The adsorption capacity of the filler (A_s, mg·m^{-2}) was calculated using the formula:

$$A_s = \frac{(C_0 - C_1)V}{mS_{\text{BET}}},$$

where m is the mass of the batch sample, g; V is the volume of the pitch solution in toluene, mL; and S_{BET} is the specific surface area of the material according to the BET method, m^2·g^{-1}.

Tribological testing and verification of the sealing performance of the finished nanocomposite samples were conducted on a high-pressure test bench designed to simulate the operation of a centrifugal pump's mechanical seal. The "graphite composite–anti-friction bronze" contact pair was

tested at a constant rotational speed of 2000 rpm in a water-alcohol mixture with a viscosity equivalent to that of the sealed liquid. To assess the material's leak tightness in the friction zone, an overpressure of 29.4 MPa was maintained, which corresponds to the extreme operating conditions of mainline equipment.

Seal tightness was assessed using a manometric method based on pressure drop in the system and detection of leaks through the seal joint. The wear rate J was calculated as a dimensionless criterion determined by the ratio of the linear wear of the sample (I_l, m), recorded by the micrometric method after running-in and reaching a steady-state friction regime, to the total sliding distance (L, m):

$$J = \frac{I_l}{L}.$$

For illustrative purposes, the characteristics of the experimental nanocomposite samples were compared with those of the most widely used sealing anti-friction material, NIGRAN-V [34].

2.4. Analytical methods

X-ray diffraction patterns of the mixture samples were recorded using an ARL Equinox 1000 diffractometer (CuKα radiation, $\lambda = 1.5406$ Å). To determine the center and half-width of the reflections, peak deconvolution was performed using OriginPro software (calculation error $\chi < 10^{-6}$). The formulas used to determine the crystal structure parameters of the samples, based on X-ray phase analysis data with references to sources, are presented in Table 1.

Table 1. Processing of the X-ray phase analysis results

Parameter	Formula	Reference
D-space, d_{002}	$d_{002} = \frac{\lambda}{2\sin\theta}$	[35]
Cohesive scattering area, L_c	$L_c = \frac{K\lambda}{\beta\cos\theta}$, where $K = 0.89$, β – half-width of a reflection	[36]
Number of layers, N	$N = \frac{L_c}{d_{002}} + 1$	[36]

The TG-DSC curves of the filler were recorded on a STA 449 F3 Jupiter (Netzsch, Germany) simultaneous thermal analyzer in air at a heating rate of 10°C/min. Mechanical compression tests were performed on an Allround Line Z250 SR Materials Testing Machine (Zwick/Roell Group). The density and open porosity of the composite samples were determined by hydrostatic weighing in isooctane ($\rho = 0.696$ g·cm^{-3}) according to the standard method (Russian Standard 2409-2014). The specific surface area (S_{BET}) was measured based on nitrogen adsorption at 77 K using an ASAP 2020 analyzer (Micromeritics, USA) via the BET method. Images of the tribocontacting surfaces of anti-friction nanocomposite products were obtained using an Axiovert metallographic microscope (Zeiss, Germany) at 20× magnification.

3. Results and Discussion

X-ray diffraction patterns of charge samples with varying graphene oxide content, compared with graphite and hexagonal boron nitride, are shown in Fig. 2.

The X-ray diffraction pattern of graphite shows a distinct reflection of the (002) crystallographic plane at $2\theta = 26.3°$. Peaks of the (100) plane at 42.7°, (101) at 44.3°, (004) at 54.2°, (112) at 83°, and (006) at 87° are also identified but are less intense.

The X-ray diffraction pattern of the boron nitride sample has a typical appearance. It shows an intense reflection from the (002) basal plane at $2\theta = 26.4°$. Peaks for the (100) plane at 41.2°, (101) at 43.4°, (102) at 49.6°, (004) at 54.6°, (110) at 76°, and (006) at 88° are also present.

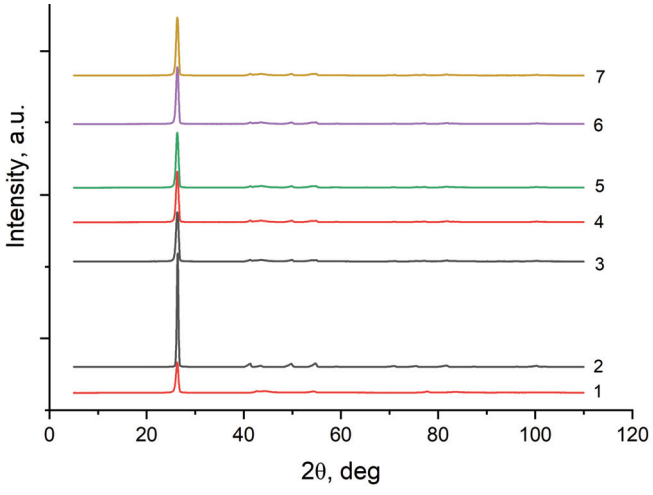

Fig. 2. X-ray diffraction patterns of graphite (*1*), hexagonal boron nitride (*2*) and charge samples containing 0 (*3*), 0.50 (*4*), 1.64 (*5*), 2.80 (*6*) and 3.66 (*7*) wt. % of graphene oxide

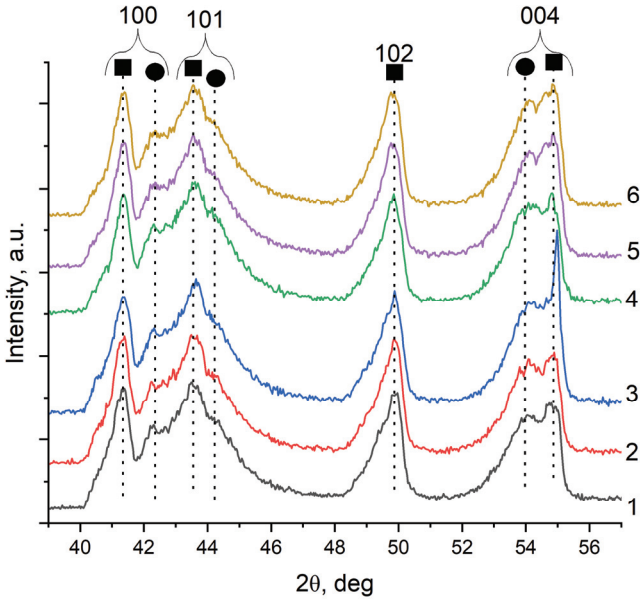

Fig. 3. Fragment of the X-ray diffraction patterns of experimental samples for the batch containing 0 (*1*), 0.50 (*2*), 1.64 (*3*), 2.80 (*4*) and 3.66 (*5*) wt. % of graphene oxide. Additional designations: ■ – boronnitride; ● – graphite

Thus, the most intense peaks on the diffraction patterns of graphite and h-BN appear virtually identical. The most distinct differences are observed in the 2θ range from 40 to 56°, which is why this specific section of the patterns of the charge samples was analyzed in greater detail (Fig. 3).

Analysis of the diffraction peaks of the experimental samples confirms that the hexagonal layered structure of the graphite and boron nitride phases is preserved during mechanical mixing in a pulverizing machine. Structural changes are most clearly observed in the second-order reflections from the (004) planes in the 54–55° range. The calculated crystal structure parameters of the experimental samples are presented in Table 2.

According to the obtained data, the introduction of GO exerts a nonlinear influence on the calculated crystallite parameters of the filler components following the cold mixing stage. The concentration dependence of both L_c and N on GO content exhibits an extremal character. At a GO content of 1.64 wt. %, the maximum values of L_c and N are observed for h-BN crystallites, suggesting ordered aggregation of this phase. In contrast, the graphite component shows the opposite trend: at the same GO concentration, its L_c and N values reach a minimum. Notably, the magnitude of these changes is substantially more pronounced for h-BN than for graphite.

It can therefore be assumed that, up to certain concentrations, GO acts as a “binding agent” for boron nitride particles, facilitating the formation of larger and more oriented stacks of h-BN layers under mechanical stress.

The decrease in the L_c and N parameters at graphene oxide concentrations above 1.64 wt. % is likely due to the fact that graphene oxide begins to act as a “dry lubricant” between the particles of the macrocomponents. As a result, the efficiency of mechanical energy transfer during grinding decreases, leading to layer disorientation and local disorder in the particle structure of the charge. The constancy of the interplanar spacing values (d_{002}) for both components suggests that during the mechanical activation process, GO does not penetrate the interlayer spaces of graphite and boron nitride, and its influence on the filler structure is due solely to surface effects.

Table 2. Results of X-ray phase analysis of the experimental samples

Component	Parameter	Values for the pure component	Values for the experimental sample with graphene oxide content, wt. %				
			0	0.5	1.64	2.8	3.66
Graphite	2θ, °	54.2	54.0	54.0	54.0	54.1	54.1
	d_{002}, Å	3.38	3.39	3.39	3.39	3.39	3.39
	L_c, Å	57.49	59.44	57.53	57.16	59.46	60.26
	N, units	18	19	18	18	19	19
Boron nitride	2θ, °	54.6	54.8	54.9	54.8	54.9	54.9
	d_{002}, Å	3.36	3.35	3.34	3.35	3.34	3.34
	L_c, Å	111.00	168.82	213.10	218.29	194.57	190.43
	N, units	34	51	65	66	59	58

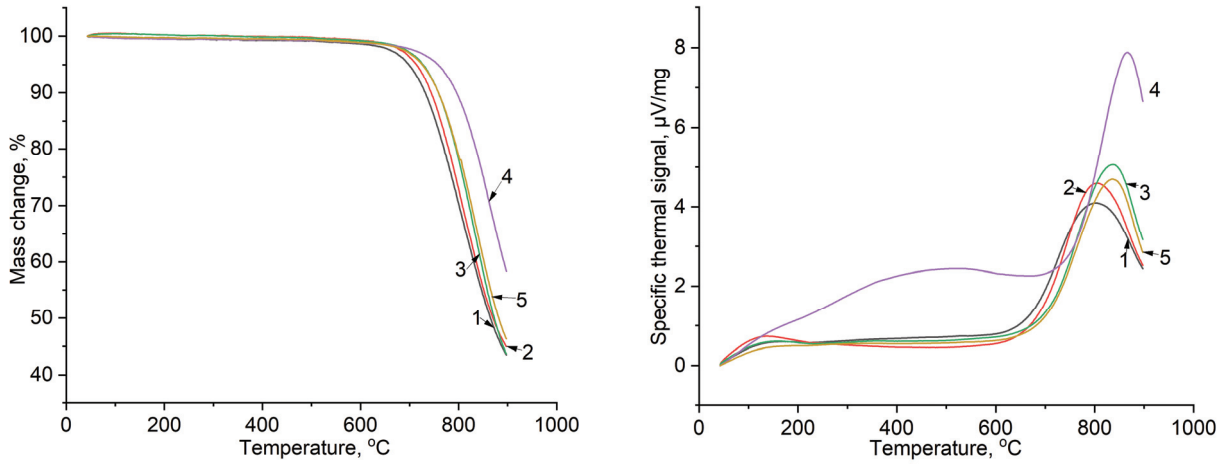

Fig. 4. TG (*a*) and DSC (b) curves of experimental samples of the batch containing 0 (*1*), 0.50 (*2*), 1.64 (*3*), 2.80 (*4*) and 3.66 (*5*) wt. % of graphene oxide

Figure 4 presents the results of simultaneous thermal analysis of the unmodified mixture and samples with different GO contents.

All studied samples remain thermally stable up to 600–650 °C, after which an intensive stage of oxidative destruction of the carbon phase begins. The effect of graphene oxide concentration on the thermal stability of the mixture is nonlinear. The sample containing 2.80 wt. % GO exhibits the highest stability, with the onset of decomposition shifted to 750 °C, whereas at other GO concentrations, decomposition begins at considerably lower temperatures. These differences in the onset temperature of thermal oxidation are likely attributable to the barrier effect of boron nitride particles, which hinder oxygen diffusion toward the graphite particles.

The DSC curves show distinct exothermic peaks in the 750–850 °C range, which corresponds to intense heat release during the oxidation of the carbon phase and confirms the thermogravimetric data on the material's decomposition. The nature of the curves suggests that the introduction of a nanomodifier affects the kinetics of the thermal oxidation process: for the sample with a content of 2.80 wt. %, the maximum heat release is shifted most to the high-temperature region. The presence of less pronounced exothermic peaks in the 100–600 °C range may be due to processes of structural rearrangement of graphene oxide or the removal of functional groups.

The properties of the final composite are significantly influenced not only by the structural but also by the textural characteristics of the filler. In this regard, as part of this work, the specific surface area (S_{BET}) values of the experimental charge samples and their adsorption capacity relative to carbon black (A_s) were determined and are presented in Table 3.

The S_{BET} dependence on GO concentration is minimal for the sample containing 1.64 % graphene oxide. Typically, materials with low specific surface areas exhibit low sorption activity. However, in this case, the sample with 1.64 % GO exhibits the maximum A_s value. Such an effect can occur only if the sorption of the pitch is specific in nature and takes place not over the entire surface of the filler, but only at active sites of a particular composition and structure. Oxygen-containing groups of graphene oxide can act as such active sites. At the optimal GO content, a filler structure is formed with the maximum number of functional groups available for the pitch sorption (Fig. 5). As the concentration of the nanomodifier (GO) increases, the filler structure is being rearranged, which contributes to a decrease in the number of active sites available for the adsorbate. This assumption is generally confirmed by the X-ray phase analysis data.

Table 3. Values of specific surface area and adsorption capacity of the filler samples

Graphene oxide content, %	S_{BET}, $m^2 \cdot g^{-1}$	A_s, $mg \cdot m^{-2}$
0	9.6	3.8
0.50	9.0	3.9
1.64	8.7	4.3
2.80	9.3	2.7
3.66	9.5	2.3

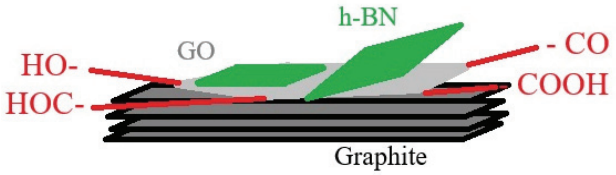

Fig. 5. Formation of a nanomodified boron nitride-graphite-graphene oxide filler

From the perspective of the composite manufacturing process, maximizing the A_s value ensures optimal wetting of the filler by the pitch binder during the hot mixing stage, which should contribute to the formation of a dense anti-friction material structure with minimal porosity.

During the next stage, the effect of the graphene oxide content in the mixture on the most important physical and mechanical properties of the experimental composite samples after the firing at 900 °C was evaluated. According to the data presented in Fig. 6, materials with a filler containing 1.64 wt. % of GO have minimum porosity and maximum compressive strength.

Thus, there is a correlation between the change in the filler structure upon modification with graphene oxide, its sorption capacity relative to the pitch, and the strength characteristics of the composite.

The best sample after firing had a porosity of 12.7 %, which is insufficient to ensure the required material impermeability. To reduce the porosity of the fired specimens, they were subjected to single and double impregnation with a furfuryl alcohol solution using the method described above, with subsequent polymerization at 300 °C.

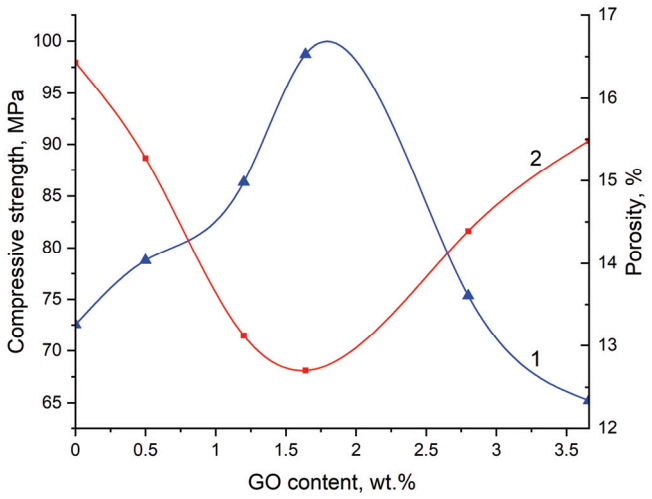

Fig. 6. The influence of graphene oxide content in the filler on the compressive strength (*1*) and porosity (*2*) of nanocomposite samples after firing at 900 °C

Table 4. Physical and mechanical properties of the finished samples of anti-friction nanocomposite in comparison with an analogous material

Number of impregnations with furfuryl alcohol solution	1	2	Analogue (NIGRAN-V)
Density, $g \cdot cm^{-3}$	1.79	1.82	1.80
Porosity, %	3.89	1.01	–
Compressive strength, MPa	–	197.5	130
Gas permeability, 10^{-5} $cm^2 \cdot s^{-1}$	107	<1	5

Thus, experimental samples of the final composite based on filler with a GO content of 1.64 wt. % were obtained. Their most important physical and mechanical properties are presented in Table 4.

After a single impregnation, the material's porosity decreases to 3.89 %, but it remains sufficiently gas-permeable. Double impregnation results in the formation of a sealed anti-friction composite that matches the density of its analogue (NIGRAN-V), has a lower gas permeability, yet its compressive strength of 197.5 MPa is 1.5 times higher than that of NIGRAN-V.

Thus, the use of GO as a charge modifier leads to the formation of a high-density and exceptionally durable material. An additional advantage lies in the relative simplicity of the nanocomposite production process. In contrast, conventionally used methods involve further processing of fired samples – comprising a product of mechanical treatment of synthetic fine-grained graphite and boron nitride bonded with pitch coke – by impregnation with coal tar pitch (softening point 65–110 °C), followed by high-temperature treatment at 1500–2050 °C and subsequent impregnation with a furfuryl alcohol solution [37].

To evaluate the developed anti-friction composite for use in sealed friction assemblies, tribotechnical bench tests were conducted on experimental samples based on both unmodified and graphene oxide-modified mixtures.

Figure 7 presents photographs of the tribologically mated surfaces of the disassembled friction assembly after testing the composites.

Following bench testing, the surface of the unmodified sample showed unacceptable defects in the form of flaking and the initiation of cracks concentric with the diameter. The observed morphological changes are indicative of fatigue failure processes occurring in the surface layer.

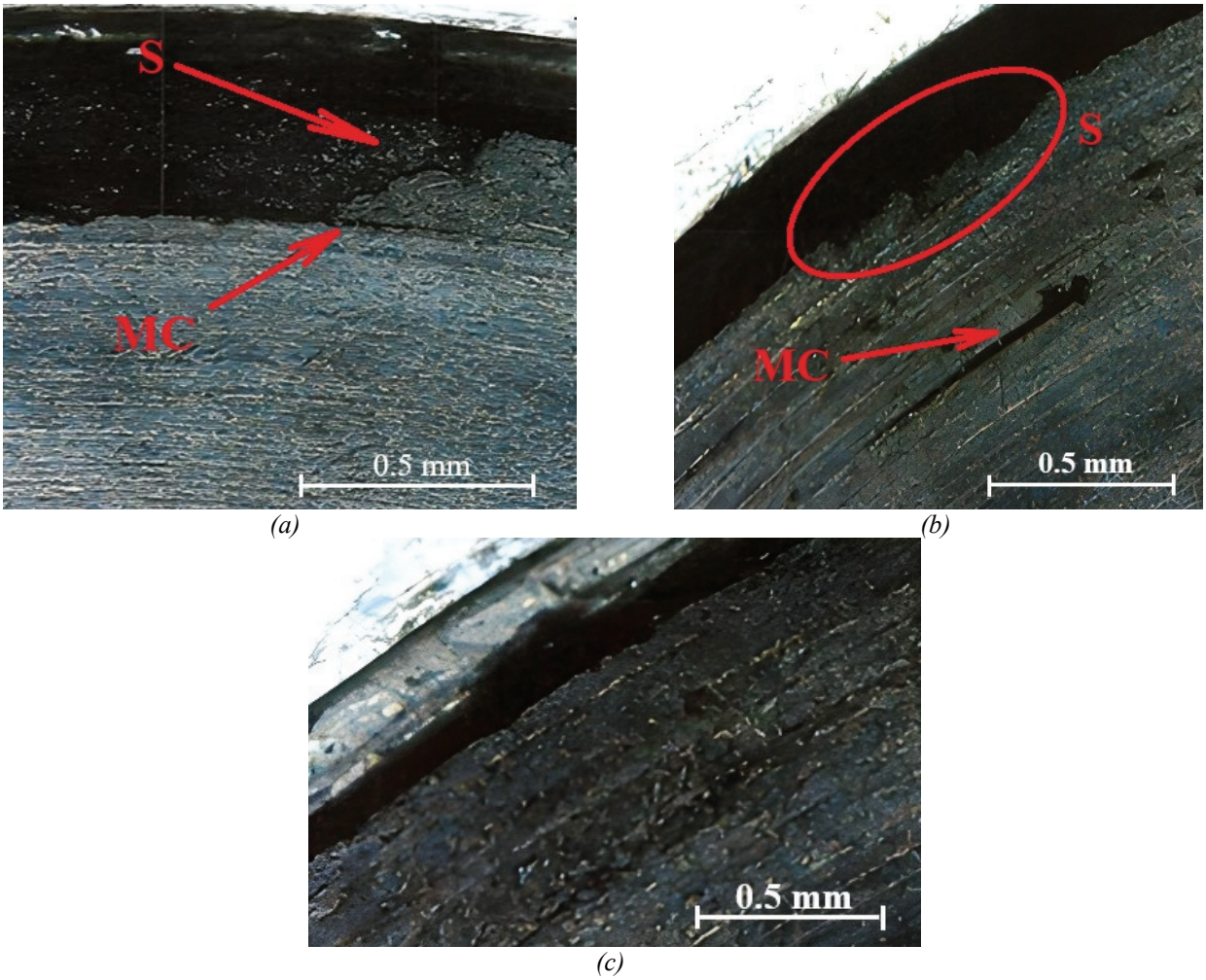

Fig. 7. Photographs of tribologically mated surfaces after testing samples of nanocomposites based on unmodified (*a*, *b*) and graphene oxide-modified (*c*) mixtures. Arrows indicate the presence of microcracks (MC) and spalling (S)

The sample based on a graphene oxide-modified mixture shows virtually no wear. Presumably, GO contributes to strengthening the bond between the filler and the binder, which is confirmed by a qualitative change in morphology after impregnation and polymerization of furfuryl alcohol (Fig. 7*c*), whereas in the control (unmodified) sample, there is a local concentration of stresses in the micropore zones (Fig. 7*a*, *b*). Under cyclic loading, these stresses trigger microcrack initiation and coalescence. The resulting crack network causes material spalling and rapid surface degradation.

Table 5. Bench test results

Graphene oxide content, wt. %	Wear rate, 10^{-9}	Seal tightness
0	59	Inleakage is observed
1.64	3.7	sealed

The data presented in Table 5 confirm the effectiveness of using GO in the composition of an anti-friction self-lubricating composite. By modifying the filler mixture, it is possible to increase the material's wear resistance by a factor of 16. Additionally, the composite retains its sealing properties even under extreme operating conditions.

4. Conclusion

This study identified key patterns in how graphene oxide influences both the formation of the matrix structure – comprising synthetic graphite and hexagonal boron nitride – and the performance properties of the resulting anti-friction composites. An addition of 1.64 wt. % graphene oxide proved critical for achieving an optimal balance of properties. At this concentration, the mixture exhibits maximum adsorption capacity for pitch, ensuring adequate wetting of the filler by the binder, which in turn facilitates the formation of a high-density matrix

with minimal open porosity. The effect of graphene oxide modification is already evident at the primary framework formation stage. Specifically, the ultimate strength of unfired samples containing 25 % graphene oxide is 25 % higher than that of the base formulation, thereby providing a structural foundation for subsequent densification. Furthermore, modifying the filler with graphene oxide, followed by impregnation with furfuryl alcohol, yielded exceptional strength characteristics due to a synergistic effect. The compressive strength reached 197.5 MPa – more than 1.5 times higher than that of the best comparable material (NIGRAN-V).

The results of tribological tests on the test bench confirmed the high effectiveness of the developed formulation. The modified composite demonstrated a nearly 16-fold reduction in wear rate compared to the base formulation, while maintaining complete sealing integrity under extreme conditions at a pressure of 29.4 MPa. Unlike unmodified samples, which are prone to fatigue spalling and the formation of main cracks, the developed material retains its structural integrity due to the strengthening effect of graphene oxide at the phase boundary. By modifying the mixture with graphene oxide, it is not only possible to obtain materials for friction components with significantly improved service life characteristics, but also to substantially simplify the manufacturing process for anti-friction composites by eliminating the stages of repeated high-temperature pitch impregnation.

5. Funding

The present study did not receive any external funding.

Финансирование

Настоящее исследование не получило внешнего финансирования.

6. Acknowledgements

This work has been done using the facilities of the shared access center “Production and Application of Multifunctional Nanomaterials” (Tambov State Technical University, Russia).

Благодарности

Работа выполнена с использованием оборудования центра коллективного пользования «Получение и применение полифункциональных наноматериалов» (Тамбовский государственный технический университет, Россия).

7. Conflict of interests

The authors declare no conflict of interest.

Конфликт интересов

Авторы заявляют об отсутствии конфликта интересов.

References

1. Chen F, Yan K, Hong J, Song J. Synergistic effect of graphene and β-Si_3N_4 whisker enables Si_3N_4 ceramic composites to obtain ultra-low friction coefficient. *Tribology International*. 2023;178:108045. DOI:10.1016/j.triboint.2022.108045

2. Nayak UP,Mücklich F, Guitar MA. Interplay between the microstructure and tribological performance of a destabilized 26 wt. % Cr HCCI: the influence of temperature and heating rate. *Tribology International.* 2023;185:108532. DOI:10.1016/j.triboint.2023.108532

3. Liu SH, Liang TH, Wang WG, Zhang BJ, et al. Tribological properties of graphene-reinforced graphite in high-temperature and high-pressure water. *Wear*. 2025;568-569:205967. DOI:10.1016/j.wear.2025.205967

4. Gong X, Chen H, Zhang F, Zhu W, et al. Degradation of tensile mechanical properties of two $Al_xCoCrFeNi$ ($x = 0.3$ and 0.4) high-entropy alloys exposed to liquid lead-bismuth eutectic at 350 and 500 °C. *Journal of Nuclear Materials*. 2022;558:153364. DOI:10.1016/j.jnucmat.2021.153364

5. Liang G, Zhang J, An S, Tang J, et al. Phase change material filled hybrid 2D/3D graphene structure with ultra-high thermal effusivity for effective thermal management. *Carbon.* 2021;176:11-20. DOI:10.1016/j.carbon.2020.12.046

6. Tofighy MA, Mohammadi T. Barrier, diffusion, and transport properties of rubber nanocomposites containing carbon nanofillers. In: *Carbon-Based Nanofillers and Their Rubber Nanocomposites*. Elsevier; 2019. p. 253-285. DOI:10.1016/B978-0-12-817342-8.00009-3

7. Wang R, Zhang F, Yang K, Xiong Y, et al. Review of two-dimensional nanomaterials in tribology: recent developments, challenges and prospects. *Advances in Colloid and Interface Science*. 2023;321:103004. DOI:10.1016/j.cis.2023.103004

8. Baiti A, Aldavud S, Algurabi A, Salhi H, et al. Modification of lubricants with graphite nanoplates. *Journal of Advanced Materials and Technologies*. 2023; 8(2):157-169. DOI:10.17277/jamt.2023.02.pp.157-169

9. Gao Q, Liu S, Hou K, Li Z, et al. Graphene-based nanomaterials as lubricant additives: a review. *Lubricants*. 2022;10(10):273. DOI:10.3390/lubricants10100273

10. Yu H, He Y, Xiao G, Fan Y, et al. The roles of oxygen-containing functional groups in modulating water purification performance of graphene oxide-based membrane. *Chemical Engineering Journal*. 2020;389:124375. DOI:10.1016/j.cej.2020.124375

11. Moazzami Gudarzi M, Sharif F. Enhancement of dispersion and bonding of graphene-polymer through wet transfer of functionalized graphene oxide. *Express Polymer*

Letters. 2012;6(12):1017-1031. DOI:10.3144/expresspolymlett.2012.107

12. Kukielski M, Kasprzak A, Zurowski R, Tanska J, et al. Functionalization of graphene oxide surface by conjugation with glucosamine and analysis of interactions occurring in nanoceramic-graphene heterostructures. *Powder Technology*. 2024;431:119089. DOI:10.1016/j.powtec.2023.119089

13. Wakchaure MB, Menezes PL. Advances in the tribological performance of graphene oxide and its composites. *Materials.* 2025;18(15):3587. DOI:10.3390/ma18153587

14. Sun J, Du S. Application of graphene derivatives and their nanocomposites in tribology and lubrication: a review. *RSC Advances*. 2019;9(69):40642-40661. DOI:10.1039/C9RA05679C

15. Ashfaq J, Channa IA, Memon AG, Chandio IA, et al. Enhancement of thermal and gas barrier properties of graphene-based nanocomposite films. *ACS Omega*. 2023;8(44):4105441063. DOI:10.1021/acsomega.3c02885

16. Bilisik K, Akter M. Polymer nanocomposites based on graphite nanoplatelets (GNPs): a review on thermal-electrical conductivity, mechanical and barrier properties. *Journal of Materials Science*. 2022;57(15):7425-7480. DOI:10.1007/s10853-022-07092-0

17. Zhao L, Peng R, Gao J, Li Y, et al. Strengthening mechanism of tribological properties of graphene oxide/multiwalled carbon nanotubes hybrid nanofluids: Molecular dynamics and experimental validation. *Journal of Colloid and Interface Science*. 2025;689:137154. DOI:10.1016/j.jcis.2025.02.162

18. Yang K, Xiong Y, Wu G, Lin H, et al. Multi-dimensional nano-additives for their superlubricity: tribological behaviors and lubrication mechanisms. *Advanced Materials Interfaces*. 2025;12(9):2400796. DOI:10.1002/admi.202400796

19. Balabanov R, Dyachkova T, Fedyushkina A, Gutnik I, et al. Influence of graphene oxide additives on the filler structure and the physical and mechanical properties of carbon-graphite nanocomposite. *Journal of Advanced Materials and Technologies.* 2025;10(1):19-31. DOI:10.17277/jamt-2025-10-01-019-031

20. Samanta S, Sahoo RR. Covalently linked hexagonal boron nitride-graphene oxide nanocomposites as high-performance oil-dispersible lubricant additives. *ACS Applied Nano Materials*. 2020;3(11):10941-10953. DOI:10.1021/acsanm.0c02193

21. Uz Zaman A, Abdul Karim MR, Hussain A, Khan MA, et al. Graphite and white graphite (h-BN) reinforced metal matrix composites and cermets: a review of processing and properties. *Advances in Materials and Processing Technologies*. 2026;12(1):222-247. DOI:10.1080/2374068X.2025.2594440

22. Yu J, Zhao W, Wu Y, Wang D, et al. Tribological properties of epoxy composite coatings reinforced with functionalized C-BN and H-BN nanofillers. *Applied Surface Science*. 2018;434:1311-1320. DOI:10.1016/j.apsusc.2017.11.204

23. Liu Y, Wang K, Xu Q, Zhang J, et al. Superlubricity between graphite layers in ultrahigh vacuum. *ACS Applied Materials & Interfaces*. 2020;12(38):43167-43172. DOI:10.1021/acsami.0c05422

24. Ouyang JH, Li YF, Zhang YZ, Wang YM, et al. High-temperature solid lubricants and self-lubricating composites: a critical review. *Lubricants*. 2022;10(8):177. DOI:10.3390/lubricants10080177

25. Srivyas PD, Charoo MS. Nano lubrication behaviour of graphite, h-BN and graphene nano platelets for reducing friction and wear. *Materials Today: Proceedings*. 2021;44:7-11. DOI:10.1016/j.matpr.2020.04.785

26. Eswaran MK, Riyas ZM, Asaithambi T. Exploring the synergistic effect of two-dimensional (2D) layered MoS2/GO/h-BN ternary nanocomposite as an electrode material for asymmetric supercapacitor application. *Journal of Materials Science: Materials in Electronics.* 2025;36(14):850. DOI:10.1007/s10854-025-14883-z

27. Zhang N, Zhang Y, Li S, Guo L, et al. 3D structurally advanced graphene oxide/h-BN hybrid for solid self-lubrication with enhanced thermal conductivity. *Tribology International*. 2022;176:107918. DOI:10.1016/j.triboint.2022.107918

28. Gupta MK, Bijwe J. Combination of nanoparticles of graphite and hexagonal boron nitride as anti-wear and extreme-pressure additives- On exploring the possibility of synergism. *Surface Topography: Metrology and Properties*. 2020;8(2):025025. DOI:10.1088/2051-672X/ab958d

29. Chen B, Dong W, Shi W, Li X, et al. Enhanced mechanical and tribological performance of epoxy nanocomposite coating by non-covalent bonded h-BN nanosheets/graphene oxide. *Progress in Organic Coatings*. 2024;197:108826. DOI:10.1016/j.porgcoat.2024.108826

30. Yang W, Luo R, Hou Z. Effect of interface modified by graphene on the mechanical and frictional properties of carbon/graphene/carbon composites. *Materials*. 2016;9(6):492. DOI:10.3390/ma9060492

31. Dhairiyasamy R, Bassi W, Algethami AA, Saleh B, et al. Advanced epoxy composites for tribological applications: investigating the role of hybrid ceramic and lubricant fillers. *Polymer Testing*. 2025;150:108932. DOI:10.1016/j.polymertesting.2025.108932

32. Li B, Zhou X, Huang J, Huang Q, et al. Investigation of multi-scale fillers on tribological properties of UHMWPE composites for water-lubricated bearings. *Tribology International*. 2025;212:110961. DOI:10.1016/j.triboint.2025.110961

33. Fan S, Zhang L, Xu Y, Cheng L, et al. Microstructure and tribological properties of advanced carbon/silicon carbide aircraft brake materials. *Composites Science and Technology*. 2008;68(14):3002-3009. DOI:10.1016/j.compscitech.2008.06.013

34. Eliseev YS, Skvortsov MA, Efremov AA, Sankin AE, Vasiliev YN. *Method for producing graphitized material*. Russian Federation patent 2,374,174 C2. 27 November 2009. (In Russ.)

35. Samoilov VM, Samsonova VB, Nakhodnova AV, Verbets DB, et al. Raman spectroscopy and crystalline structure of polyacrylonitrile-based carbon fibres. *Advanced Materials & Technologies*. 2019;3(15):008-015. DOI:10.17277/amt.2019.03.pp.008-015

36. Memetova A, Tyagi I, Rao Karri R, Suhas, et al. High-density nanoporous carbon materials as storage material for methane: A value-added solution. *Chemical Engineering Journal*. 2022;433:134608. DOI:10.1016/j.cej.2022.134608

37. Pankov MI, Kulakov VV, Lavruhin SP, Luchkin MS. *Method for producing self-lubricating material based on artificial finegrained graphite*. Russian Federation patent 2,748,329 C1. 24 May 2021. (In Russ.)

Information about the authors / Информация об авторах

Roman D. Balabanov, Postgraduate Student, Tambov State Technical University (TSTU), Tambov, Russian Federation; ORCID 0009-0001-2946-3119; e-mail: balabanoff98@gmail.com

Tatyana P. Dyachkova, D. Sc. (Chem.), Professor, TSTU, Tambov, Russian Federation; ORCID 0000-0002-4884-5171; e-mail: dyachkova_tp@mail.ru

Irina V. Gutnik, Cand. Sc. (Eng.), Associate Professor, TSTU, Tambov, Russian Federation; ORCID 0000-0003-1236-7187; e-mail: i.v.gutnik@yandex.ru

Nikolay A. Chapaksov, Cand. Sc. (Eng.), Associate Scientist, TSTU, Tambov, Russian Federation; ORCID 0000-0001-9076-9400; e-mail: tchapaxov.nikolaj@yandex.ru

Elena A. Burakova, D. Sc. (Eng.), Associate Professor, TSTU, Tambov, Russian Federation; ORCID 0000-0001-8927-7433; e-mail: elenburakova@yandex.ru

Балабанов Роман Дмитриевич, аспирант, Тамбовский государственный технический университет (ТГТУ), Тамбов, Российская Федерация; ORCID 0009-0001-2946-3119; e-mail: balabanoff98@gmail.com

Дьячкова Татьяна Петровна, доктор химических наук, профессор, ТГТУ, Тамбов, Российская Федерация; ORCID 0000-0002-4884-5171; e-mail: dyachkova_tp@mail.ru

Гутник Ирина Владимировна, кандидат технических наук, доцент, ТГТУ, Тамбов, Российская Федерация; ORCID 0000-0003-1236-7187; e-mail: i.v.gutnik@yandex.ru

Чапаксов Николай Андреевич, кандидат технических наук, младший научный сотрудник, ТГТУ, Тамбов, Российская Федерация; ORCID 0000-0001-9076-9400; e-mail: tchapaxov.nikolaj@yandex.ru

Буракова Елена Анатольевна, доктор технических наук, доцент, ТГТУ, Тамбов, Российская Федерация; ORCID 0000-0001-8927-7433; e-mail: elenburakova@yandex.ru

Received 19 March 2026; Revised 24 April 2026; Accepted 28 April 2026